The Effect of Source Size on the Buildup Factor Calculation of Absolute Volume

Jeffry A. Siegel

Department of Diagnostic Imaging, Division of Nuclear Medicine, Temple University Hospital, Philadelphia, Pennsylvania

A general scheme for generating attenuation-corrected images for use in absolute volume measurements has been developed. The technique is based on a buildup factor approach for Compton scatter compensation and requires anterior and posterior count-rate measurements. The scatter correction requires evaluation of the attenuation factor $(1-(1-e^{-\mu d})^{B(\infty)}$, where μ is the linear attenuation coefficient in cm^{-1} and $B(\infty)$ is the buildup factor at infinite depth. The attenuation factors for four different source sizes using $^{99m}TcO_4^-$ and a 20% scintillation camera energy window are reported. The results indicated that $B(\infty)$ was constant while μ varied as a function of size (S) in pixels according to $\mu = 0.151\ cm^{-1} \times \exp(-1.18 \times 10^{-4}\ pixels^{-1} \times S)$. Once the appropriate value of μ was determined, a pair of anterior-posterior count rate equations was used to generate attenuation-corrected count rate data for use in absolute volume measurements. The method was validated by calculating three separate phantom volumes. The results showed that the method provides less than $\pm 6.0\%$ error for volume determinations at all investigated depths.

J Nucl Med 26:1319–1322, 1985

Conventional nuclear medicine images contain a significant amount of scattered radiation due to the relatively wide energy window settings employed. Count-based algorithms for measuring absolute volumes are influenced by attenuation and tissue scatter which is present due to the inherent broad-beam conditions of the measurement. A buildup factor technique (*1-4*) was recently introduced in order to develop a general methodology for scatter compensation.

In this article we have investigated the dependence of absolute volume measurements on the depth-independent buildup factor (*4*) as a function of source size for a constant scintillation camera energy window setting. A general scheme for scatter correction in planar imaging is presented.

MATERIALS AND METHODS

A scintillation camera fitted with a low-energy, parallel-hole collimator and interfaced to a commercial nuclear medicine computer system was employed for these studies. The camera was peaked for technetium-99m (^{99m}Tc) with a 20% energy window. Four thin circular sources (~0.2 cm) of diameters 3.7 cm, 6.0 cm, 8.5 cm and 13.6 cm were prepared containing 700 μCi (26 MBq) each of [^{99m}Tc]pertechnetate. These sources were counted in air at 10 cm from the collimator face and at multiple depths in a 30 × 30 × 20 cm phantom of tissue equivalent material (Mix D). Computer generated regions of interest (ROI) were then used to obtain all the source count rates for the transmission factor determination.

The transmission factor (TF) is calculated according to:

$$TF = C/C_o, \quad (1)$$

where

C = count rate measured for source at depth d in phantom

C_o = count rate measured in air for same source-to-collimator distance.

The TF data for all four source sizes were analyzed by a nonlinear least-squares fitting routine using the function (*4*):

$$TF = 1-(1-e^{-\infty d})^{B(\infty)}, \quad (2)$$

where

μ = linear attenuation coefficient in cm^{-1}; d = source depth in cm; $B(\infty)$ = buildup factor at infinite depth.

Received Mar. 12, 1985; revision accepted July 19, 1985.

For reprints contact: Jeffry A. Siegel, PhD, Section of Nuclear Medicine, Temple University Hospital, 3401 North Broad St., Philadelphia, PA 19140.

Three separate cylindrical volume sources of water containing [^{99m}Tc]pertechnetate were then prepared [source 1: 150 ml, 5 cm thick, cross-sectional area of 30.2 cm^2, 1.3 mCi (44 MBq); source 2: 150 ml, 4 cm thick, cross-sectional area of 37.4 cm^2 1 mCi (37 MBq); source 3: 400 ml, 2.6 cm thick, cross-sectional area of 153.9 cm^2, 1.2 mCi (44 MBq)]. These sources were positioned at various depths in the tissue-equivalent material. Anterior and posterior count rates were obtained and a 10 ml aliquot was taken from each of the three volume sources and counted in air at 10 cm from the collimator by the same camera-collimator system in the appropriate size petri dish. The count rates were determined in all cases using a semiautomated edge detection algorithm (MUGE, Medical Data Systems). The volumes were then calculated for depths from 3 to 10 cm.

The volume determination is based upon the equation, volume = C/C_{alq}, where C_o is the attenuation-corrected source count rate and C_{alq} is the 10 ml aliquot count rate per ml. In order to determine C_o we used our previously reported depth-independent buildup factor technique (*4*). Essentially, the method consists of setting up separate anterior (C_A) and posterior (C_P) count rate equations according to:

$$C_A = C_o\,[1-(1-e^{-\mu A^d})^{B(\infty)}] \times [\sinh(\mu_A x/2)/(\mu_A x/2)]$$
$$C_P = C_o\,[1-(1-e^{-\mu P^{(T-d)}})^{B(\infty)}] \times [\sinh(\mu_P x/2)/(\mu_P x/2)] \quad (3)$$

where $1-(1-e^{-\mu d})^{B(\infty)}$ is the transmission factor obtained from equation 2, μ_A and μ_P are the linear attenuation coefficients for the anterior and posterior images, respectively, x is the source thickness in cm, T is the total phantom thickness in cm, and the sinh term is the source self-attenuation correction.

Equation 3 can be combined to give:

$$C_A/C_P = \frac{1-(1-e^{-\mu A^d})^{B(\infty)}}{1-(1-e^{-\mu P^{(T-d)}})^{B(\infty)}} \quad (4)$$

The self-attenuation terms of Eqs. 3 are assumed to cancel out. This approximation results in at most a 2% error. Equation 4 is solved numerically for depth d by varying the value of d under the constraint $0 \le d \le T$. Either part of Eq. (3) can then be used to calculate C_o for use in the volume equation (volume = C_o/C_{alq}). A computer algorithm was written in BASIC to facilitate data analysis.

RESULTS

The measured transmission factors (TF) are plotted versus depth d for the two extreme source sizes in Fig. 1. These curves are not simple exponentials but consist of an initial shoulder region followed by an exponential portion. The results of the nonlinear least-squares fit (according to Eq. 2) to these data are shown in Table 1. The buildup factor at infinite depth, B(∞), appeared to have

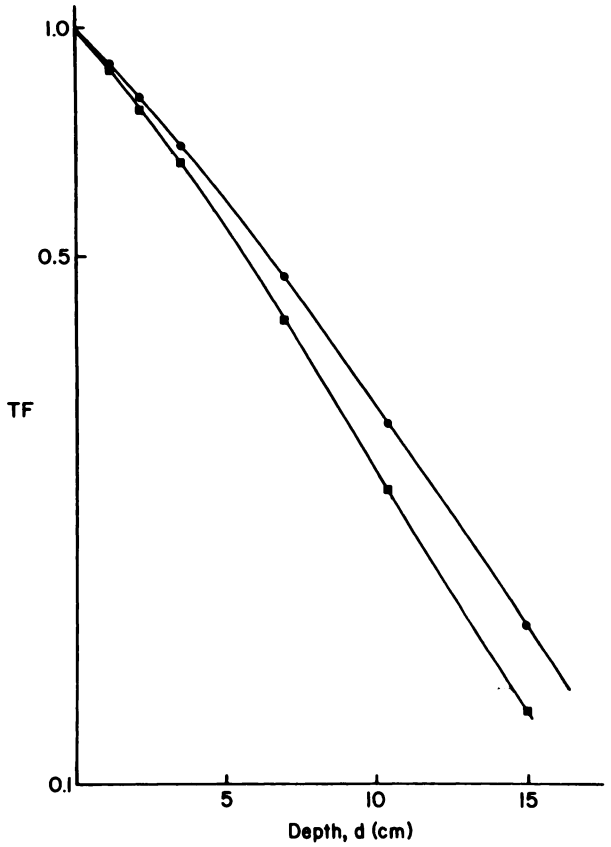

FIGURE 1
Transmission factor, TF, as function of depth obtained in phantom of tissue-equivalent material for two source sizes. Other two sources (diameters of 6.0 cm and 8.5 cm) fell between these results and were omitted for clarity. (●) 13.6 cm; (■) 3.7 cm

no systematic dependence on source diameter (or ROI size) and its average value was found to be 1.23. The linear attenuation coefficient μ is seen to vary as a function of ROI size. This dependence was found to be in the form of

$$\mu = \mu_o \times e^{-k(\text{ROIsize})} \quad (5)$$

where ROI size is the number of pixels in the circular source ROI, μ_o = 0.151 cm^{-1} and k = 1.18 × 10^{-4} pixels^{-1}. The results were obtained by pseudolinear regression analysis with a correlation coefficient of –0.97 and a standard error of the estimate equal to 0.016 cm^{-1}. The parameter μ_o represents the linear attenuation coefficient for an infinitely small source and is in excellent agreement with previously reported values for the narrow beam μ (5).

The transmission factor data was also analyzed using the counts observed in the total field of view (or whole-frame counts) instead of the ROI counts as discussed above. The results of the curve fitting resulted in constant values for the parameters μ and B(∞) for all four source sizes. The linear attenuation coefficient μ was 0.120 cm^{-1}

TABLE 1
Results of Curve Fit to Function
$TF = 1-(1-e^{-\mu d})^{B(\infty)}$

Source [diam. (cm)]	ROI size*	Parameter		Chi-square†
		μ	B(∞)	
3.7	170 ± 3	0.150 ± 0.001	1.21 ± 0.01	1.7
6.0	330 ± 4	0.146 ± 0.001	1.27 ± 0.01	4.8
8.5	511 ± 5	0.140 ± 0.001	1.21 ± 0.01	6.6
13.6	1,215 ± 11	0.132 ± 0.001	1.21 ± 0.01	16.5

*This corresponds to average number of pixels ± 1 s.d. in source ROI at all investigated depths.
†Chi-square is normalized to number of degrees of freedom.

TABLE 2
Results of Volume Determination

	Volume source					
	1*		2†		3‡	
Anterior depth (cm)	Calculated depth (cm)	Volume (% error)	Calculated depth (cm)	Volume (% error)	Calculated depth (cm)	Volume (% error)
3	3.3	143 (-4.7)	3.1	151 (0.7)	2.7	376 (-6.0)
4	4.2	144 (-4.0)	4.1	153 (2.0)	3.8	381 (-4.8)
5	5.2	146 (-2.7)	5.1	154 (2.7)	4.8	377 (-5.8)
6	6.1	147 (-2.0)	6.2	154 (2.7)	5.9	380 (-5.0)
7	7.1	148 (-1.3)	7.1	157 (4.7)	6.9	384 (-4.0)
8	8.1	148 (-1.3)	8.1	157 (4.7)	8.0	387 (-3.3)
9	9.1	149 (-0.7)	9.1	156 (4.0)	8.9	386 (-3.5)
10	10.0	149 (-0.7)	10.0	155 (3.3)	10.0	384 (-4.0)

*Volume source 1: 150 ml, 355 ± 5 pixels in ROI.
†Volume source 2: 150 ml, 398 ± 6 pixels in ROI.
‡Volume source 3: 400 ml, 1320 ± 9 pixels in ROI.

and B(∞) was 1.15. This value for μ is in agreement with the values reported by other investigators (*6*). However, the whole-frame count approach has limited application for use in patient data analysis since there is no mechanism for isolation of individual organ count rate information.

The results of the absolute volume quantitation are shown in Table 2. The appropriate values for the linear attenuation coefficients μ_A and μ_P for use in Eq. (3) were obtained based upon the ROI size of the volume sources according to Eq. 5. Since the ROI sizes were essentially constant for each volume source at all investigated depths (Table 2), their average values were used resulting in the same value for μ_A and μ_P. The errors in the volume measurement for all three volume sources ranged from +4.7% to -6.0%. The anterior depth determinations obtained by Eq. (4) are also shown in Table 2.

The conventional method for volume determination also uses the equation, volume = C_o/C_{alq}, however, C_o is simply given by $C_A/e^{-\mu d}$ where C_A is the anterior count rate and μ is the linear attenuation coefficient taken to be 0.15 cm^{-1}. For comparison with the buildup factor analysis, we can use this conventional technique to determine the volume of source 1 (Table 2) at 8 cm depth. In this case C_A was 90,000 counts and C_{alq} was 1634 counts. Therefore, the volume = $90{,}000/(e^{-0.15\times8} \times 1{,}634)$ = 183 ml, representing overestimation of 22%.

DISCUSSION

Compton scattered photons are a fact of life for nuclear medicine image formation due to its inherent broad-beam nature. The scattered photons are a result of the relatively wide energy window settings (20–25%) which must be employed clinically in order to shorten imaging time. These photons thus serve a useful purpose and do not usually significantly degrade image quality. However, if quantitative analysis is desired the effects of scatter must be taken into account.

The equation $TF = 1-(1-e^{-\mu d})^{B(\infty)}$ provides the key for deriving attenuation correction factors. As has been shown B(∞) is independent of source size and depth for a given window setting. Since the linear attenuation coefficient μ varies with source size, i.e., number of pixels in the ROI, given any source size, the values for μ to be used in the pair of anterior-posterior count rate equations [Eq. (3)] can be derived. The following procedure can be employed: determine the number of pixels in the ROI from

the anterior and posterior count rate images, and then calculate the correct μ values to be used in Eq. (3) based upon the obtained ROI sizes according to Eq. 5.

We previously reported that $B(\infty)$, not μ, varied as a function of source sizes (*4*). However, those results were obtained using data from different imaging systems and we noted that the source size dependence could therefore not be accurately determined. Nevertheless, from the energy window setting information also obtained and the present study we can discern two distinct trends. As the energy window is increased with a constant source size (*4*), μ remains constant while $B(\infty)$ increases. Secondly, as the source size is increased with a constant energy window setting, $B(\infty)$ remains constant while μ decreases. This is exactly what theory would predict concerning the behavior of the buildup factor which is defined as the infinite depth scatter correction. The scatter cutoff is fixed for a given window setting, [constant $B(\infty)$], and will change as a function of window setting [variable $B(\infty)$] since more or less scatter will be included.

We have previously indicated (*4*) that the equation $TF = 1-(1-e^{-\mu d})^{B(\infty)}$ should replace the commonly used attenuation or transmission factor relationship of $TF = e^{-\mu d}$. This latter relationship indicates that a semilogarithmic plot of TF versus depth would be linear. This is simply not true as evidenced by Figure 1 and our other reported results (*2, 4, 7*) due to the relatively wide energy window settings employed in clinical nuclear medicine imaging. The linear approximation is only valid as the window setting approaches zero since the width of the shoulder region will decrease (*4*). However, narrow window settings are not clinically useful on a routine basis since they would result in inordinately long imaging times. Furthermore, the considerable buildup effect, 20–25% in this case, is completely ignored by $e^{-\mu d}$ leading to potentially significant errors. The controversy concerning the proper choice of μ, 0.15 cm^{-1} compared with a more appropriate value of 0.11-0.12 cm^{-1} when using the equation $TF = e^{-\mu d}$ is, therefore, superfluous.

The buildup factor approach can easily be adapted for use in clinical nuclear medicine images. Differences in the anterior and posterior size and shape of any ROI can be accounted for in terms of attenuation and scatter through the use of Eq. (5). The average patient thickness, T, required for the measurement will compensate for count rates even when the patient thickness varies within the region of interest. The counts rates C_A and C_P are net count rates and therefore, must be corrected for background (*3*). THe buildup factor approach has already been applied clinically for ventricular volume determinations (*3*) and dosimetry calculations (*8*).

In conclusion, a general scheme for attenuation correction has been developed. Once the constant $B(\infty)$ and μ as a function of source size are known for a constant energy window setting, the appropriate values of the linear attenuation coefficient can easily be calculated for any source size. These values can then be used in the pair of anterior-posterior count rate equations [Eq. (3)] to obtain attenuation-corrected data for use in absolute volume determinations.

REFERENCES

1. Siegel JA, Wu RK: The elusive buildup factor. *Med Phys* 9:614, 1982 (abstr)
2. Wu RK, Siegel JA: Absolute quantitation of radioactivity using the buildup factor. *Med Phys* 11:189-192, 1984
3. Siegel JA, Maurer AH, Wu RK, et al: Absolute left ventricular volume by an iterative buildup factor analysis of gated radionuclide images. *Radiology* 151:477-481, 1984
4. Siegel JA, Wu RK, Maurer AH: The buildup factor: Effect of scatter on absolute volume determination. *J Nucl Med:* in press
5. John HE, Cunningham JR: *The Physics of Radiology,* Illinois, Charles C. Thomas, Third Edition, 1977, p 746
6. Harris CC, Greer KL, Jaszczak RJ, et al: Tc-99m attenuation coefficients in water-filled phantoms determined with gamma cameras. *Med Phys* 11:681-685, 1984
7. Siegel JA, Maurer AH: Estimation of absolute ventricular volume. *Chest* 85:711, 1984 (lett)
8. Wu RK, Siegel JA, Rattner Z, et al: Tc-99m HIDA dosimetry in patients with various hepatic disorders. *J Nucl Med* 25:905-912, 1984